Research Article

Unsteady Squeezing Flow of Casson Fluid with Magnetohydrodynamic Effect and Passing through Porous Medium

Hamid Khan,[1] Mubashir Qayyum,[1] Omar Khan,[2] and Murtaza Ali[3]

[1]*Department of Mathematics, National University of Computer and Emerging Sciences, Peshawar, Pakistan*
[2]*Department of Computer Sciences, National University of Computer and Emerging Sciences, Peshawar, Pakistan*
[3]*Department of Basic Sciences and Humanities, University of Engineering and Technology, Peshawar, Pakistan*

Correspondence should be addressed to Hamid Khan; hamid.khan@nu.edu.pk

An unsteady squeezing flow of Casson fluid having magnetohydrodynamic (MHD) effect and passing through porous medium channel is modeled and investigated. Similarity transformations are used to convert the partial differential equations (PDEs) of non-Newtonian fluid to a highly nonlinear fourth-order ordinary differential equation (ODE). The obtained boundary value problem is solved analytically by Homotopy Perturbation Method (HPM) and numerically by explicit Runge-Kutta method of order 4. For validity purpose, we compare the analytical and numerical results which show excellent agreement. Furthermore, comprehensive graphical analysis has been made to investigate the effects of various fluid parameters on the velocity profile. Analysis shows that positive and negative squeeze number S_q have opposite effect on the velocity profile. It is also observed that Casson parameter β shows opposite effect on the velocity profile in case of positive and negative squeeze number S_q. MHD parameter M_g and permeability constant M_p have similar effects on the velocity profile in case of positive and negative squeeze numbers. It is also seen that, in case of positive squeeze number, similar velocity profiles have been obtained for β, M_g, and M_p. Besides this, analysis of skin friction coefficient has also been presented. It is observed that squeeze number, MHD parameter, and permeability parameter have direct relationship while Casson parameter has inverse relationship with skin friction coefficient.

1. Introduction

Squeezing flow between parallel plates is an important problem in the area of fluid dynamics. The problem can be described akin to the principle of moving pistons, where the squeezing behavior of two parallel plates produces a flow that is normal to the plates. Applications of the problem are found in hydraulic machinery and tools, electric motors, food industry, bioengineering, and automobile engines. Other simpler but equally important examples are flow patterns occurring in syringes and compressible tubes. In these applications, flow patterns can be classified into laminar, turbulent, and transitional flows on the basis of the well-known Reynold's number. From an industrial perspective, it is necessary to study the effect of these different behaviors for non-Newtonian fluids, the mechanics of which have proved

to be a significant challenge to the research community. The non-Newtonian fluid model being considered in our case is that of Casson [1, 2] as it is able to capture complex rheological properties of a fluid, unlike other simplified models like the powerlaw [3] and grade-two or grade-three [4] models. Concentrated fluids like sauces, honey, juices, blood, and printing inks [5] can be well described using this model. More formally, Casson fluid can be defined as a shear thinning liquid which is assumed to have an infinite viscosity at zero rate of shear, a yield stress below which no flow occurs, and a zero viscosity at an infinite rate of shear [6]. Application of Casson fluid for flow between two rotating cylinders is performed in [7]. In some industrial applications, the model has to deal with conducting fluids which exhibit different behaviors under the influence of a magnetic field. In these cases, the magnetohydrodynamic

(MHD) aspect of the flow needs to be considered. In this article, we investigate this particular case for a porous medium channel and present a comprehensive analysis. To the best of our knowledge, this particular case has not been addressed before. A porous medium, identified as a material that contains fluid-filled pores, is always characterized by properties such as porosity and permeability. Porosity defines the quantity of fluid that can be held by the material, whereas permeability is the amount of fluid that can pass through it. Various applications include ground water hydrology, chemical reactors, irrigation, drainage, seepage, and recovery of crude oil from pores of reservoir rocks [8–12]. These applications can specifically be classified to engineering fields such as petroleum, reservoir, and chemical engineering.

Due to the nonlinearity of the model under consideration, exact solutions are rarely found in body of literature and, if found, involve simplified assumptions. For this purpose, many analytical approximation techniques are used instead [13, 14]. The usual approach for boundary value problems is the usage of perturbation techniques. However, due to assumptions of small or large parameters, this is not sufficient. In this regard, a seminal work that combined these perturbation techniques with homotopy was proposed as the Homotopy Perturbation Method (HPM) in [15–17]. Since its introduction, the method has been applied to different nonlinear equations [18–22]. Specifically in the case of fluid dynamics, the method has been applied in [18–20, 23]. The classical HPM has also been modified by few researchers [24, 25]. Other approximation techniques that have been used for the case of fluid dynamics include the Homotopy Analysis Method (HAM) [26], Optimal Homotopy Asymptotic Method (OHAM) [27], Adomian Decomposition Method (ADM) [28], and Variational Iteration Method (VIM) [29]. In addition to these analytical approaches, various numerical schemes can also be used to solve these problems. Examples are the family of Runge-Kutta [30], finite difference [31], and wavelet methods.

In the remaining part of the manuscript, Section 2 includes mathematical formulation of the problem. Sections 3 and 4 present the basic theory of HPM and its application to Casson fluid model. Section 5 comprises the results and discussion. Finally, conclusion is presented in Section 6.

2. Mathematical Formulation

An incompressible flow of Casson fluid is considered between two parallel plates that have been separated by a distance $z = \pm l(1 - \alpha t)^{1/2} = \pm h(t)$. Here, l is the initial gap between the two plates at time t, and α is the squeezing motion of both plates. Both plates touch one another at $t = a/\alpha$. $\alpha < 0$ implies a receding motion of the plates. With these conditions, the non-Newtonian Casson fluid, using [32, 33], is defined as

$$
\tau_{ij} = \begin{cases} 2\left[\mu_B + \dfrac{P_y}{2\pi}\right]e_{ij}, & \pi > \pi_c, \\ 2\left[\mu_B + \dfrac{P_y}{2\pi_c}\right]e_{ij}, & \pi_c > \pi, \end{cases} \tag{1}
$$

where τ_{ij} is the (i, j)th component of the stress tensor, $\pi = e_{ij}e_{ij}$, e_{ij} being the (i, j)th component of the deformation rate, π_c is the critical value of the material, μ_B is plastic dynamic viscosity, and P_y is the yield stress of the fluid. A constant magnetic field of strength M_g is applied perpendicularly and relatively fixed to the walls. It is assumed that the intensity of the effective field produced due to the conducting fluid is negligible and that there is no other external electric field. The governing relation for flow under these assumptions is given as

$$
\frac{\partial u_x}{\partial x} + \frac{\partial u_y}{\partial y} = 0, \tag{2}
$$

$$
\frac{\partial u_x}{\partial t} + u_x \frac{\partial u_x}{\partial x} + u_y \frac{\partial u_x}{\partial y}
$$
$$
= -\frac{1}{\rho}\frac{\partial p}{\partial x} + \nu\left(1 + \frac{1}{\beta}\right)\left(2\frac{\partial^2 u_x}{\partial x^2} + \frac{\partial^2 u_x}{\partial y^2} + 2\frac{\partial^2 u_y}{\partial y \partial x}\right) \tag{3}
$$
$$
- \frac{\sigma B^2}{\rho}u_x - \frac{\mu}{\rho k}u_x,
$$

$$
\frac{\partial u_y}{\partial t} + u_x \frac{\partial u_y}{\partial x} + u_y \frac{\partial u_y}{\partial y}
$$
$$
= -\frac{1}{\rho}\frac{\partial p}{\partial y} + \nu\left(1 + \frac{1}{\beta}\right)\left(2\frac{\partial^2 u_y}{\partial x^2} + \frac{\partial^2 u_y}{\partial y^2} + 2\frac{\partial^2 u_x}{\partial y \partial x}\right) \tag{4}
$$
$$
- \frac{\mu}{\rho k}u_y,
$$

where u_x and u_y are the velocity components in x and y directions, p is the pressure, μ and ν are the viscosity and kinematic viscosity of the fluid, $\beta = \mu_B\sqrt{2\pi/P_y}$ is the Casson fluid parameter, B is the magnitude of the imposed magnetic field, and k is the permeability constant. The boundary conditions for the problem are given as follows:

$$
u_x = 0,
$$
$$
u_y = v_w = \frac{dh}{dt} \quad \text{at } y = h(t),
$$
$$
\frac{\partial u_x}{\partial y} = 0, \tag{5}
$$
$$
u_y = 0 \quad \text{at } y = 0.
$$

Cross differentiating (3) and (4) and by introducing the vorticity function ω, we get

$$
\frac{\partial \omega}{\partial t} + u_x \frac{\partial \omega}{\partial x} + u_y \frac{\partial \omega}{\partial y} = \nu\left(1 + \frac{1}{\beta}\right)\left(\frac{\partial^2 \omega}{\partial x^2} + \frac{\partial^2 \omega}{\partial y^2}\right)
$$
$$
- \frac{\sigma B^2}{\rho}\frac{\partial u_x}{\partial y} - \frac{\mu}{\rho k}\omega, \tag{6}
$$

where

$$
\omega = \left(\frac{\partial u_y}{\partial x} - \frac{\partial u_x}{\partial y}\right). \tag{7}
$$

The similarity transform for a two-dimensional flow [34] is

$$u_x = \frac{\alpha x}{2(1 - \alpha t)} U'(\eta),$$

$$u_y = \frac{-\alpha l}{2(1 - \alpha t)^{1/2}} U(\eta),$$

(8)

where $\eta = y/[l(1 - \alpha t)^{1/2}]$. Substituting (8) into (6) using (7) gives the following nonlinear differential equation that describes Casson's fluid flow:

$$\left(1 + \frac{1}{\beta}\right) \frac{d^4 U(\eta)}{d\eta^4} - S_q \left[\eta U(\eta) + 3\frac{d^2 U(\eta)}{d\eta^2}\right.$$

$$\left. + \frac{dU(\eta)}{d\eta} \frac{d^2 U(\eta)}{d\eta^2} - U(\eta) \frac{d^3 U(\eta)}{d\eta^3}\right] - M_g \frac{d^2 U(\eta)}{d\eta^2}$$

$$- M_p \frac{d^2 U(\eta)}{d\eta^2} = 0,$$

(9)

where $S_q = \alpha l^2/(2\nu)$ is the nondimensional squeeze number that describes movement of the plates. $S_q > 0$ corresponds to the plates moving apart, while $S_q < 0$ corresponds to the collapsing movement. Using (8), the boundary conditions for the problem are reduced to

$$U(0) = 0,$$

$$U''(0) = 0,$$

$$U(1) = 1,$$

$$U'(1) = 0.$$

(10)

When $M_g = M_p = 0$ and $\beta \to \infty$, the current problem is reduced to the problem discussed in [34].

The skin friction coefficient is defined as [35]

$$C_f = \nu \left(1 + \frac{1}{\beta}\right) \frac{(\partial u_x/\partial y)_{y=h(t)}}{v_w^2}.$$

(11)

In terms of (8), we have

$$\frac{l^2}{x^2(1 - \alpha t)\,\mathrm{Re}_x C_f} = \left(1 + \frac{1}{\beta}\right) U''(1),$$

(12)

where $\mathrm{Re}_x = 2l v_w^2/[\nu x(1 - \alpha t)^{1/2}]$.

3. Basic Theory of Homotopy Perturbation Method

The basic theory of HPM can be exhibited using the following differential equation:

$$L(w) + N(w) - g(r) = 0, \quad r \in \Omega,$$

$$B\left(w, \frac{dw}{dn}\right) = 0, \quad r \in \Upsilon,$$

(13)

where w is an unknown and $g(r)$ is a known function, L, N, B are linear, nonlinear, and boundary operators, and Υ is the boundary of the domain Ω. A homotopy $\theta(r, p) : \Omega \times [0, 1] \to \mathbb{R}$ is then constructed which satisfies

$$\psi(\theta, p) = (1 - p)[L(\theta) - L(w_0)]$$

$$+ p[L(\theta) + N(\theta) - g(r)] = 0, \quad r \in \Omega,$$

(14)

where $p \in [0, 1]$ is an embedding parameter and w_0 is the initial guess which satisfies the boundary conditions. From (14), we have

$$\psi(\theta, 0) = L(\theta) - L(w_0) = 0,$$

$$\psi(\theta, 1) = L(\theta) + N(\theta) - g(r) = 0.$$

(15)

Thus, as p varies from 0 to 1, the solution $\theta(r, p)$ approaches from $w_0(r)$ to $\widetilde{w}(r)$. To obtain an approximate solution, we expand $\theta(r, p)$ in a Taylor series about p as follows:

$$\theta(r, p) = \theta_0 + \sum_{k=1}^{\infty} \theta_k p^k.$$

(16)

Setting $p = 1$, the approximate solution of (25) would be

$$\widetilde{U} = \lim_{p \to 1} \theta(r, p) = \sum_{k=1}^{\infty} \theta_k.$$

(17)

Substituting (17) into (13) will give

$$R(x) = L[\widetilde{U}(x)] + N[\widetilde{U}(x)] - f(x).$$

(18)

If $R = 0$, then $\widetilde{U}$ will be the exact solution but usually this does not happen in nonlinear problems.

4. Implementation of HPM to Squeezing Flow of Casson Fluid

Using (9) and (10), various-order problems are presented as follows.

Zeroth-order problem is

$$U_0^{(iv)}(\eta) + \frac{1}{\beta} U_0^{(iv)}(\eta) = 0,$$

$$U_0(0) = 0,$$

$$U_0''(0) = 0,$$

$$U_0(1) = 1,$$

$$U_0'(1) = 0.$$

(19)

Solution of the zeroth order problem is

$$U_0(\eta) = \frac{1}{2}\left(3\eta - \eta^3\right).$$

(20)

First-order problem is

$$\frac{1}{\beta}U_1^{(iv)}(\eta) + U_1^{(iv)}(\eta) - S_q\eta U_0(\eta) - M_pU_0''(\eta)$$

$$- M_gU_0''(\eta) - 3S_qU_0''(\eta) - S_qU_0'(\eta)U_0''(\eta)$$

$$+ S_qU_0(\eta)U_0'''(\eta) = 0,$$

$$U_1(0) = 0,$$

$$U_1''(0) = 0,$$

$$U_1(1) = 0,$$

$$U_1'(1) = 0.$$

$$(21)$$

Solution of the first-order problem is

$$U_1(\eta) = -\frac{1}{6720(1+\beta)}\left(\Phi_{11}\eta - \Phi_{12}\eta^3 + \Phi_{13}\eta^5\right.$$

$$\left. - \Phi_{14}\eta^6 - \Phi_{15}\eta^7 + \Phi_{16}\eta^8\right).$$

$$(22)$$

Second-order problem is

$$U_2^{(iv)}(\eta) + \frac{1}{\beta}U_2^{(iv)}(\eta) - S_q\eta U_1(\eta) - S_qU_1'(\eta)U_0''(\eta)$$

$$- M_pU_1''(\eta) - M_gU_1''(\eta) - 3S_qU_1''(\eta)$$

$$- S_qU_0'(\eta)U_1''(\eta) + S_qU_1(\eta)U_0'''(\eta)$$

$$+ S_qU_0(\eta)U_1'''(\eta),$$

$$U_2(0) = 0,$$

$$U_2''(0) = 0,$$

$$U_2(1) = 0,$$

$$U_2'(1) = 0.$$

$$(23)$$

Solution of the second-order problem is

$$U_2(\eta) = -\frac{1}{9686476800(1+\beta)^2}\left[\Phi_{21}\eta + \Phi_{22}\eta^3\right.$$

$$+ \Phi_{23}\eta^5 + \Phi_{24}\eta^6 + \Phi_{25}\eta^7 + \Phi_{26}\eta^8 + \Phi_{27}\eta^9$$

$$\left. + \Phi_{28}\eta^{10} - \Phi_{29}\eta^{11} + \Phi_{210}\eta^{12} + \Phi_{211}\eta^{13}\right],$$

$$(24)$$

where $\Phi_1 i$ and $\Phi_2 j$ are the coefficients of various powers of η. These coefficients are given in the Appendix for the reader convenience.

In a similar way, higher order problems can be formulated and solved. These approximations have been excluded from the manuscript for brevity purpose.

Considering the third-order solution,

$$\widetilde{U}(\eta) = \sum_{j=0}^{3}U_j(\eta).$$

$$(25)$$

By fixing values of β, S_q, M_g, and M_p in (25) polynomial solution can be found. For instance, when $\beta = 0.01$, $S_q = -0.2$, $M_g = 0.5$, and $M_p = 0.5$, the third-order solution is therefore

$$\widetilde{U}(\eta) = \begin{cases} 0.0 + 1.49988\eta - 0.499762\eta^3 - 0.0000989628\eta^5 - 8.25014 \times 10^{-6}\eta^6 \\ -7.08874 \times 10^{-6}\eta^7 + 5.87168 \times 10^{-7}\eta^8 - 2.33686 \times 10^{-9}\eta^9 \\ +1.61604 \times 10^{-10}\eta^{10} + 4.40191 \times 10^{-11}\eta^{11} - 4.96322 \times 10^{-12}\eta^{12} \\ -3.44636 \times 10^{-14}\eta^{13} - 3.72105 \times 10^{-15}\eta^{14} - 1.04633 \times 10^{-15}\eta^{15} \\ +1.29806 \times 10^{-16}\eta^{16} + 2.11403 \times 10^{-19}\eta^{17} + 1.83374 \times 10^{-21}\eta^{18}. \end{cases}$$

$$(26)$$

The residual error of the problem is

$$\text{RE} = \left(1 + \frac{1}{\beta}\right)\frac{d^4\widetilde{U}}{d\eta^4}$$

$$- S_q\left[\eta\widetilde{U} + 3\frac{d^2\widetilde{U}}{d\eta^2} + \frac{d\widetilde{U}}{d\eta}\frac{d^2\widetilde{U}}{d\eta^2} - \widetilde{U}\frac{d^3\widetilde{U}}{d\eta^3}\right]$$

$$- M_g\frac{d^2\widetilde{U}}{d\eta^2} - M_p\frac{d^2\widetilde{U}}{d\eta^2}.$$

$$(27)$$

5. Results and Discussion

In this article, an unsteady squeezing flow of Casson fluid having MHD effect and passing through porous medium channel is considered. Four parameters are considered here: the squeeze number S_q, Casson parameter β, MHD parameter M_g, and the permeability parameter M_p. The resulting boundary value problem is solved for various values of the mentioned parameters using HPM and the results are compared with numerical solutions obtained using explicit Runge-Kutta method of order 4 (ERK4). Tables 4–7 shows the comparison of analytical and numerical solutions along with residual errors for various values of fluid parameters. A quick
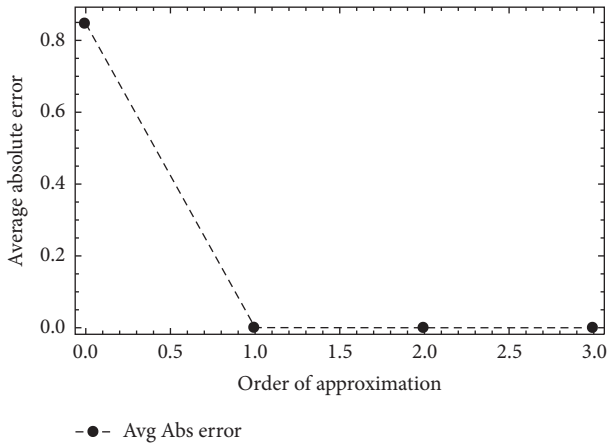
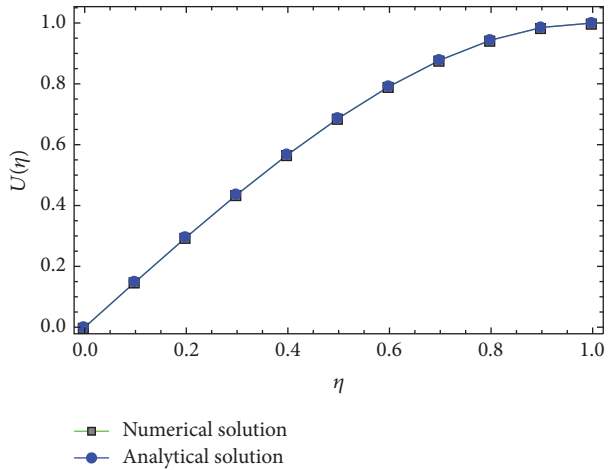FIGURE 1: Convergence of homotopy perturbation solution.

FIGURE 2: Comparison of analytical and numerical solutions.

TABLE 1: Skin friction coefficient for various values of fluid parameters.

S_q	β	M_g	M_p	$\left(1+\dfrac{1}{\beta}\right)U''(1)$
−8.0	0.5	1.0	1.0	−2.144
−6.0		1.0	1.0	−4.919
−3.0		1.0	1.0	−7.728
−0.6	0.05	0.5	0.5	−62.922
−0.2			1.5	−63.307
			1.7	−63.347
	0.01		0.5	−303.108
	0.1			−33.107
	0.3			−13.108
	0.4			−10.608
	0.5			−9.108
	0.8			−6.858
	1.0			−6.108
	0.05	0.1		−63.563
		0.7		−63.147
		1.2		−63.247
0.2	0.01	0.5		−303.292
	0.3			−13.287
	0.4			−10.786
	0.05		1.4	−63.470
			1	−63.390
0.6			0.5	−63.473
0.8				−63.563
1.0	0.5	1.0	1.0	−9.785
2.0				−10.130
4.0				−10.756
	1.0			−7.731
	3.0			−5.969
	5.0			−5.722
	8.0			−5.620
8.0	0.5			−12.310
3.0	1.0	1.0		−7.381
		4.0		−7.862
		8.0		−8.542
5.0		1.0	0.1	−7.998
			5.0	−8.972
			10	−10.146

analysis of these tables reveals that the results from HPM are consistent and in good agreement with the numerical results.

The convergence of the homotopy solution is confirmed by finding various-order solutions along with absolute residual errors in Table 2. Here, it can be observed that the HPM solution improves considerably as the order of approximation is increased. The validity of analytical solution based on HPM is checked by comparing it with numerical solutions of ERK4 in Table 3. Here, $M_g = 0.5$, $\beta = 0.05$, and the squeeze number is varied as $-0.2 \leq S_q \leq 0.6$. Validity is confirmed for all variations of squeeze number. Both the convergence and validity are also demonstrated graphically in Figures 1 and 2.

Numerical values of skin friction coefficients corresponding to various fluid parameters are given in Table 1. Analysis of these numerical quantities show that increase in β decreases the skin friction coefficient. Furthermore, increase in S_q, M_g, and M_p increases the skin friction coefficient. It is also observed that increase in M_g and M_p increases the skin friction coefficient.

The effects of identified parameters on the velocity profile are illustrated graphically in Figures 3–10. The effect of negative S_q on the velocity profile is shown in Figure 3, where it is shown that the normal velocity profile increases with the increase in negative S_q. On the other hand, the radial velocity increases near the lower plate and terminates near the upper plate. It can also be observed that, for fixed values of fluid parameters, the normal velocity monotonically increases while the radial velocity monotonically decreases. Moreover, the radial velocity increases when $0 < \eta \leq 0.45$ and decreases when $0.45 < \eta \leq 1$.

In the next three figures, the effect of various fluid parameters on the velocity profile with $S_q < 0$ is depicted. First, the effect of Casson parameter β is shown in Figure 4, showing that the normal velocity increases as β is increased,

TABLE 2: Various-order homotopy perturbation solutions along with absolute residual errors for fixed values of fluid parameters.

η	Zeroth order		First order		Second order		Third order	
	Solution	Error	Solution	Error	Solution	Error	Solution	Error
0.0	0.0	0.0	0.0	0.0	0.0	0.0	0.0	0.0
0.1	0.1495	0.12395	0.149488	5.58×10^{-5}	0.149488	6.38×10^{-9}	0.149488	8.92×10^{-13}
0.2	0.296	0.25664	0.295977	1.03×10^{-4}	0.295977	7.98×10^{-9}	0.295977	2.45×10^{-12}
0.3	0.4365	0.40239	0.436469	1.30×10^{-4}	0.436469	1.13×10^{-9}	0.436469	4.63×10^{-12}
0.4	0.568	056384	0.567965	1.25×10^{-4}	0.567965	1.52×10^{-8}	0.567965	6.20×10^{-12}
0.5	0.6875	074375	0.687464	7.15×10^{-5}	0.687464	3.76×10^{-8}	0.687464	4.79×10^{-12}
0.6	0.792	094464	0.791969	5.16×10^{-5}	0.791969	5.52×10^{-8}	0.791969	1.91×10^{-12}
0.7	0.8785	1.16879	0.878477	2.67×10^{-4}	0.878477	4.70×10^{-8}	0.878477	1.37×10^{-11}
0.8	0.944	1.41824	0.943987	6.05×10^{-4}	0.943987	2.20×10^{-8}	0.943987	2.36×10^{-11}
0.9	0.9855	1.69479	0.985496	1.09×10^{-3}	0.985496	2.05×10^{-7}	0.985496	1.05×10^{-11}
1.0	1.0	2.0	1.0	1.78×10^{-3}	1.0	5.77×10^{-7}	1.0	6.93×10^{-11}

TABLE 3: Comparison of analytical and numerical solution for various S_q.

η	|ERK4 − HPM|					
	$M_p = M_g = 0.5, \ \beta = 0.05$					
	$S_q = -0.2$	$S_q = -0.4$	$S_q = -0.6$	$S_q = 0.2$	$S_q = 0.4$	$S_q = 0.6$
0.0	0.0	0.0	0.0	0.0	0.0	0.0
0.1	8.32×10^{-15}	5.77×10^{-14}	6.37×10^{-12}	2.12×10^{-11}	9.52×10^{-11}	2.80×10^{-10}
0.2	1.38×10^{-14}	1.10×10^{-13}	1.20×10^{-11}	3.94×10^{-11}	1.77×10^{-10}	5.23×10^{-10}
0.3	1.38×10^{-14}	1.52×10^{-13}	1.63×10^{-11}	5.21×10^{-11}	2.36×10^{-10}	6.97×10^{-10}
0.4	7.38×10^{-15}	1.78×10^{-13}	1.88×10^{-11}	5.77×10^{-11}	2.63×10^{-10}	7.80×10^{-10}
0.5	4.44×10^{-15}	1.85×10^{-13}	1.90×10^{-11}	5.56×10^{-11}	2.55×10^{-10}	7.61×10^{-10}
0.6	1.68×10^{-14}	1.70×10^{-13}	1.70×10^{-11}	4.65×10^{-11}	2.16×10^{-10}	6.48×10^{-10}
0.7	2.37×10^{-14}	1.32×10^{-13}	1.29×10^{-11}	3.27×10^{-11}	1.54×10^{-10}	4.65×10^{-10}
0.8	1.97×10^{-14}	7.87×10^{-14}	7.63×10^{-12}	1.75×10^{-11}	8.42×10^{-11}	2.55×10^{-10}
0.9	7.67×10^{-15}	2.53×10^{-14}	2.49×10^{-12}	5.13×10^{-12}	2.50×10^{-11}	7.68×10^{-11}
1.0	1.24×10^{-19}	1.10×10^{-16}	1.11×10^{-16}	2.57×10^{-21}	6.86×10^{-22}	4.98×10^{-19}

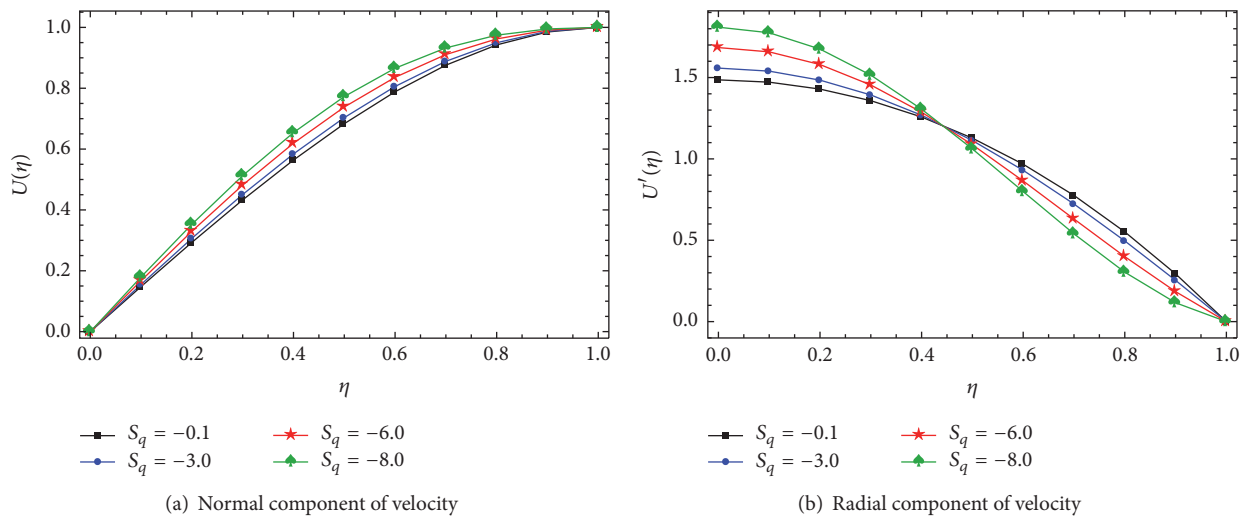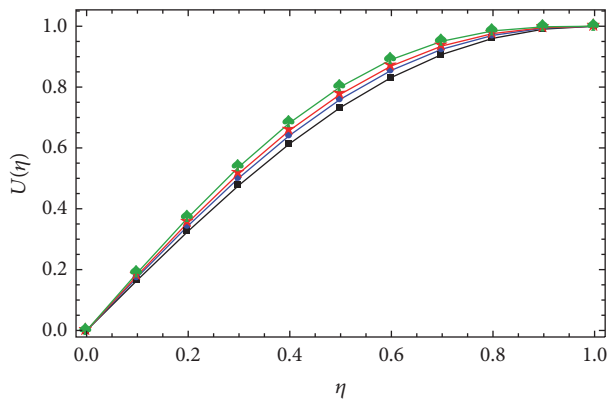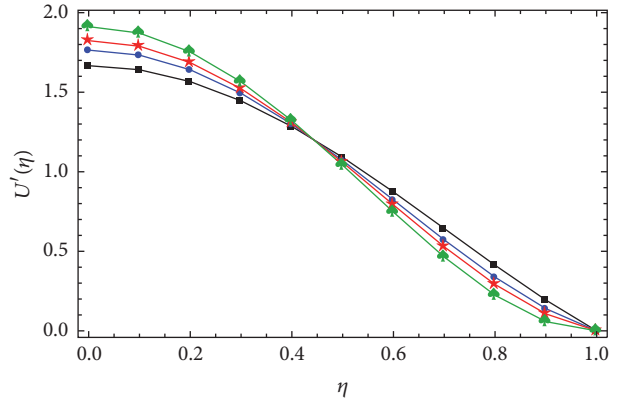(a) Normal component of velocity

(b) Radial component of velocity

FIGURE 3: Effect of negative squeeze number S_q on the velocity profile.

TABLE 4: Solutions along with residual errors for various S_q when $M_g = M_p = 0.5$, $\beta = 0.05$.

Parameter	η	Solution		Residual error	
		HPM	ERK4	HPM	ERK4
$S_q = -0.2$	0.0	0.0	0.0	0.0	1.40×10^{-7}
	0.1	0.149441	0.149441	9.93×10^{-11}	6.59×10^{-9}
	0.2	0.29589	0.29589	2.73×10^{-10}	-1.35×10^{-9}
	0.3	0.436351	0.436351	5.16×10^{-10}	2.71×10^{-10}
	0.4	0.567829	0.567829	6.89×10^{-10}	-2.04×10^{-10}
	0.5	0.687329	0.687329	5.33×10^{-10}	2.41×10^{-10}
	0.6	0.791849	0.791849	-2.13×10^{-10}	-8.42×10^{-11}
	0.7	0.878387	0.878387	-1.53×10^{-9}	-5.29×10^{-10}
	0.8	0.943935	0.943935	-2.63×10^{-9}	2.65×10^{-9}
	0.9	0.985479	0.985479	-1.17×10^{-9}	-1.08×10^{-8}
	1.0	1.0	1.0	7.72×10^{-9}	-1.50×10^{-7}
$S_q = -0.4$	0.0	0.0	0.0	0.0	7.25×10^{-7}
	0.1	0.1495	0.1495	-5.03×10^{-11}	3.68×10^{-8}
	0.2	0.295999	0.295999	-9.77×10^{-11}	-8.75×10^{-9}
	0.3	0.436497	0.436497	-1.52×10^{-10}	2.33×10^{-9}
	0.4	0.567995	0.567995	-2.62×10^{-10}	-7.32×10^{-10}
	0.5	0.687493	0.687493	-5.45×10^{-10}	-5.65×10^{-12}
	0.6	0.791991	0.791991	-1.15×10^{-9}	6.91×10^{-10}
	0.7	0.878491	0.878491	-2.09×10^{-9}	-1.86×10^{-9}
	0.8	0.943994	0.943994	-2.85×10^{-9}	6.26×10^{-9}
	0.9	0.985498	0.985498	-1.81×10^{-9}	-2.54×10^{-8}
	1.0	1.0	1.0	4.49×10^{-9}	-4.34×10^{-7}
$S_q = -0.6$	0.0	0.0	0.0	0.0	1.61×10^{-6}
	0.1	0.149558	0.149558	-1.24×10^{-8}	8.03×10^{-8}
	0.2	0.296108	0.296108	-2.49×10^{-8}	-1.93×10^{-8}
	0.3	0.436644	0.436644	-3.79×10^{-8}	5.07×10^{-9}
	0.4	0.568161	0.568161	-5.28×10^{-8}	-1.55×10^{-9}
	0.5	0.687657	0.687657	-7.21×10^{-8}	3.17×10^{-10}
	0.6	0.792134	0.792134	-9.99×10^{-8}	1.06×10^{-9}
	0.7	0.878596	0.878596	-1.42×10^{-7}	-4.49×10^{-9}
	0.8	0.944053	0.944053	-2.06×10^{-7}	1.61×10^{-8}
	0.9	0.985561	0.985561	-3.01×10^{-7}	-6.40×10^{-8}
	1.0	1.0	1.0	-4.33×10^{-7}	-1.05×10^{-6}

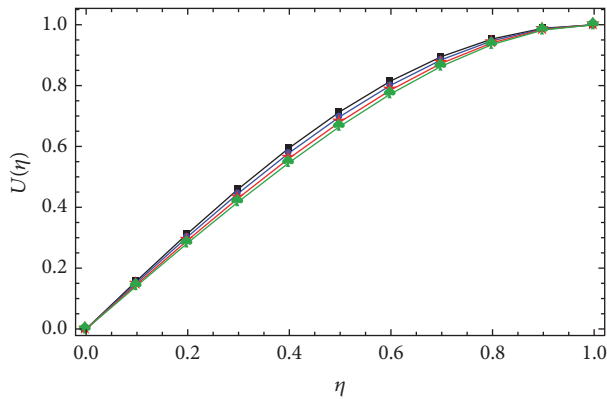(a) Normal component of velocity

(b) Radial component of velocity

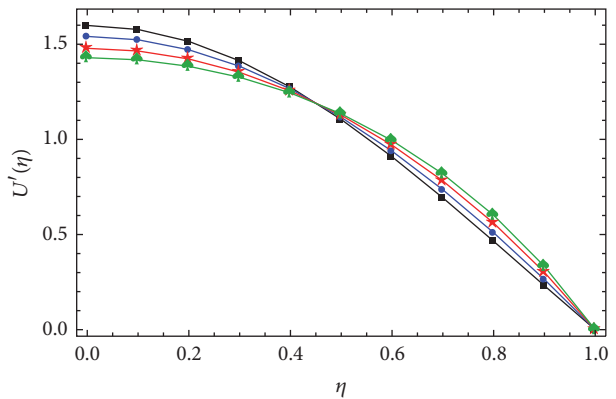FIGURE 4: Effect of Casson parameter β on the velocity profile when S_q is negative.

TABLE 5: Solutions along with residual errors for various β when $M_g = M_p = 0.5$, $S_q = -0.2$.

Parameter	η	Solution		Residual error	
		HPM	ERK4	HPM	ERK4
$\beta = 0.01$	0.0	0.0	0.0	0.0	-1.76×10^{-7}
	0.1	0.149488	0.149502	8.92×10^{-13}	-8.33×10^{-9}
	0.2	0.295977	0.296004	2.45×10^{-12}	4.75×10^{-9}
	0.3	0.436469	0.436506	4.63×10^{-12}	-2.87×10^{-9}
	0.4	0.567965	0.568006	6.20×10^{-12}	-3.59×10^{-10}
	0.5	0.687464	0.687506	4.79×10^{-12}	2.45×10^{-9}
	0.6	0.791969	0.792005	-1.91×10^{-12}	-1.50×10^{-9}
	0.7	0.878477	0.878504	-1.37×10^{-11}	-1.89×10^{-9}
	0.8	0.943987	0.944002	-2.36×10^{-11}	8.25×10^{-9}
	0.9	0.985496	0.985501	-1.05×10^{-11}	-2.78×10^{-8}
	1.0	1.0	1.0	6.93×10^{-11}	-3.31×10^{-7}
$\beta = 0.1$	0.0	0.0	0.0	0.0	3.51×10^{-7}
	0.1	0.149388	0.149522	6.91×10^{-10}	1.83×10^{-8}
	0.2	0.295789	0.296041	1.90×10^{-9}	-4.39×10^{-9}
	0.3	0.436215	0.436554	3.59×10^{-9}	1.08×10^{-9}
	0.4	0.567674	0.568059	4.79×10^{-9}	-2.68×10^{-10}
	0.5	0.687173	0.687557	3.71×10^{-9}	-2.80×10^{-11}
	0.6	0.791712	0.792048	-1.48×10^{-9}	2.99×10^{-10}
	0.7	0.878285	0.878533	-1.06×10^{-8}	-8.24×10^{-10}
	0.8	0.943876	0.944018	-1.83×10^{-8}	2.81×10^{-9}
	0.9	0.985461	0.985505	-8.20×10^{-9}	-1.16×10^{-8}
	1.0	1.0	1.0	5.37×10^{-8}	-1.95×10^{-7}
$\beta = 0.2$	0.0	0.0	0.0	0.0	6.28×10^{-7}
	0.1	0.149295	0.14954	4.25×10^{-9}	3.03×10^{-8}
	0.2	0.295614	0.296075	1.17×10^{-8}	-7.38×10^{-9}
	0.3	0.435977	0.436599	2.21×10^{-8}	2.07×10^{-9}
	0.4	0.567403	0.568109	2.95×10^{-8}	-7.36×10^{-10}
	0.5	0.686901	0.687605	2.28×10^{-8}	1.63×10^{-10}
	0.6	0.791472	0.792087	-9.14×10^{-9}	4.70×10^{-10}
	0.7	0.878105	0.878561	-6.57×10^{-8}	-1.87×10^{-9}
	0.8	0.943773	0.944032	-1.12×10^{-7}	6.77×10^{-9}
	0.9	0.985428	0.985509	-5.05×10^{-8}	-2.73×10^{-8}
	1.0	1.0	1.0	3.31×10^{-7}	-4.47×10^{-7}

(a) Normal component of velocity
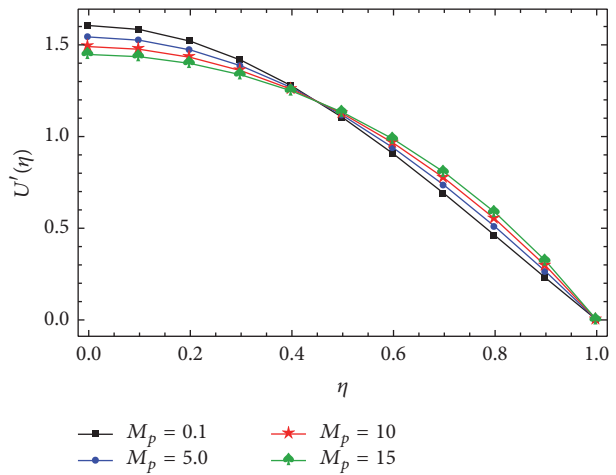
(b) Radial component of velocity

FIGURE 5: Effect of MHD parameter M_g on the velocity profile when S_q is negative.

TABLE 6: Solutions along with residual errors for various M_g when $M_p = 0.5$, $S_q = -0.2$, $\beta = 0.05$.

Parameter	η	Solution		Residual error	
		HPM	ERK4	HPM	ERK4
	0.0	0.0	0.0	0.0	1.73×10^{-7}
	0.1	0.149372	0.149488	-3.30×10^{-8}	1.73×10^{-7}
	0.2	0.29576	0.295977	-6.29×10^{-8}	-2.10×10^{-9}
	0.3	0.436177	0.436469	-8.69×10^{-8}	4.10×10^{-10}
	0.4	0.567634	0.567964	-1.02×10^{-7}	-7.13×10^{-11}
$M_g = 0.1$	0.5	0.687137	0.687463	-1.08×10^{-7}	5.99×10^{-11}
	0.6	0.791684	0.791966	-1.02×10^{-7}	-1.65×10^{-11}
	0.7	0.878267	0.878474	-8.46×10^{-8}	-3.51×10^{-10}
	0.8	0.943868	0.943985	-5.38×10^{-8}	1.99×10^{-9}
	0.9	0.985459	0.985459	-9.68×10^{-9}	-9.11×10^{-9}
	1.0	1.0	1.0	4.83×10^{-8}	-1.24×10^{-7}
	0.0	0.0	0.0	0.0	8.57×10^{-8}
	0.1	0.149338	0.149453	-7.57×10^{-8}	1.30×10^{-9}
	0.2	0.295695	0.295912	-1.43×10^{-7}	-2.14×10^{-10}
	0.3	0.436089	0.43638	-1.95×10^{-7}	7.59×10^{-11}
	0.4	0.567534	0.567863	-2.26×10^{-7}	-3.50×10^{-10}
$M_g = 0.4$	0.5	0.687037	0.687362	-2.31×10^{-7}	5.60×10^{-10}
	0.6	0.791597	0.791878	-2.08×10^{-7}	-2.96×10^{-10}
	0.7	0.878202	0.878409	-1.55×10^{-7}	-7.90×10^{-10}
	0.8	0.943831	0.943947	-7.53×10^{-8}	3.92×10^{-9}
	0.9	0.985447	0.985483	3.09×10^{-8}	-1.56×10^{-8}
	1.0	1.0	1.0	1.59×10^{-7}	-2.04×10^{-7}
	0.0	0.0	0.0	0.0	1.28×10^{-7}
	0.1	0.149268	0.149383	-2.69×10^{-7}	4.96×10^{-9}
	0.2	0.295564	0.29578	-5.05×10^{-7}	-1.04×10^{-9}
	0.3	0.435913	0.436203	-6.78×10^{-7}	3.68×10^{-10}
	0.4	0.567334	0.567662	-7.64×10^{-7}	-4.53×10^{-10}
$M_g = 1.0$	0.5	0.686833	0.687162	-7.49×10^{-7}	2.64×10^{-10}
	0.6	0.791422	0.791703	-6.25×10^{-7}	3.42×10^{-10}
	0.7	0.878073	0.878279	-3.99×10^{-7}	-8.95×10^{-10}
	0.8	0.943757	0.943873	-8.61×10^{-8}	1.28×10^{-9}
	0.9	0.985424	0.98546	2.89×10^{-7}	-2.79×10^{-9}
	1.0	1.0	1.0	6.93×10^{-7}	-9.05×10^{-8}
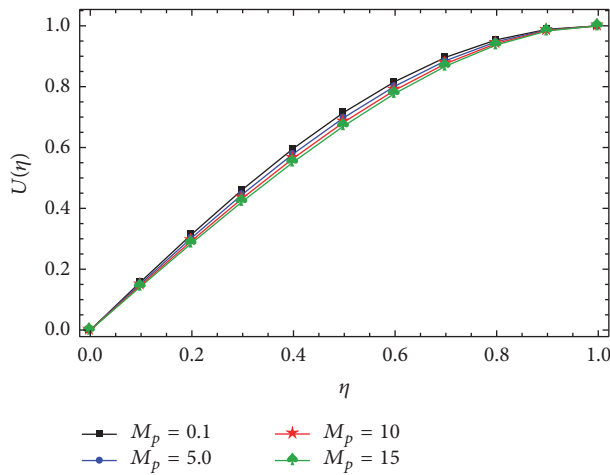
(a) Normal component of velocity

(b) Radial component of velocity

FIGURE 6: Effect of permeability constant M_p on the velocity profile when S_q is negative.

TABLE 7: Solutions along with residual errors for various M_p when $M_g = 0.5$, $S_q = -0.2$, $\beta = 0.05$.

Parameter	η	Solution		Residual error	
		HPM	ERK4	HPM	ERK4
	0.0	0.0	0.0	0.0	1.28×10^{-7}
	0.1	0.149383	0.149383	-2.87×10^{-9}	4.96×10^{-9}
	0.2	0.29578	0.295978	-4.06×10^{-9}	-1.04×10^{-9}
	0.3	0.436203	0.436203	-2.56×10^{-9}	3.68×10^{-10}
	0.4	0.567662	0.567662	1.37×10^{-9}	-4.53×10^{-10}
$M_p = 1.0$	0.5	0.687162	0.687162	6.02×10^{-9}	2.64×10^{-10}
	0.6	0.791703	0.791703	8.52×10^{-9}	3.42×10^{-10}
	0.7	0.878279	0.878279	6.00×10^{-9}	-8.95×10^{-10}
	0.8	0.943873	0.943873	-2.25×10^{-9}	1.28×10^{-9}
	0.9	0.98546	0.98546	-1.14×10^{-8}	-2.79×10^{-9}
	1.0	1.0	1.0	-6.12×10^{-9}	-9.05×10^{-8}
	0.0	0.0	0.0	0.0	5.71×10^{-8}
	0.1	0.149325	0.149325	-2.60×10^{-8}	1.22×10^{-10}
	0.2	0.295671	0.295671	-4.28×10^{-8}	1.00×10^{-10}
	0.3	0.436056	0.436056	-4.40×10^{-8}	8.10×10^{-11}
	0.4	0.567495	0.567495	-2.82×10^{-8}	-3.44×10^{-10}
$M_p = 1.5$	0.5	0.686995	0.686995	-3.16×10^{-10}	4.62×10^{-10}
	0.6	0.791558	0.791558	2.87×10^{-8}	-2.07×10^{-10}
	0.7	0.878171	0.878171	4.50×10^{-8}	-6.54×10^{-10}
	0.8	0.943812	0.943812	3.74×10^{-8}	3.13×10^{-9}
	0.9	0.985441	0.985441	7.51×10^{-9}	-1.22×10^{-8}
	1.0	1.0	1.0	-1.60×10^{-8}	-1.62×10^{-7}
	0.0	0.0	0.0	0.0	1.58×10^{-7}
	0.1	0.149302	0.149302	-4.79×10^{-8}	1.08×10^{-8}
	0.2	0.295627	0.295627	-8.04×10^{-8}	-2.34×10^{-9}
	0.3	0.435997	0.435997	-8.64×10^{-8}	2.54×10^{-10}
	0.4	0.567428	0.567428	-6.27×10^{-8}	1.88×10^{-10}
$M_p = 1.7$	0.5	0.686929	0.686929	-1.60×10^{-8}	-7.14×10^{-11}
	0.6	0.791499	0.791499	3.70×10^{-8}	-8.03×10^{-11}
	0.7	0.878128	0.878128	7.43×10^{-8}	-1.19×10^{-10}
	0.8	0.943787	0.943787	7.58×10^{-8}	1.11×10^{-9}
	0.9	0.985433	0.985433	3.80×10^{-8}	-4.87×10^{-9}
	1.0	1.0	1.0	-5.44×10^{-9}	-6.74×10^{-8}

(a) Normal component of velocity

(b) Radial component of velocity
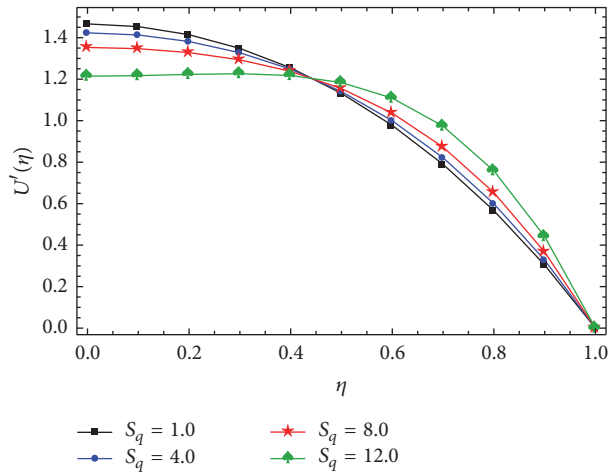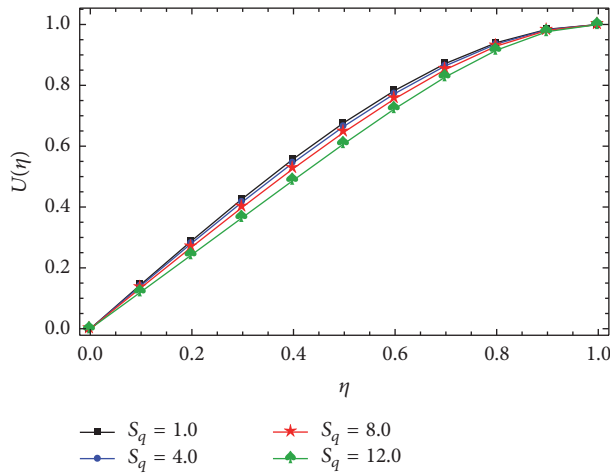
FIGURE 7: Effect of positive squeeze number S_q on the velocity profile.

(a) Normal component of velocity

(b) Radial component of velocity
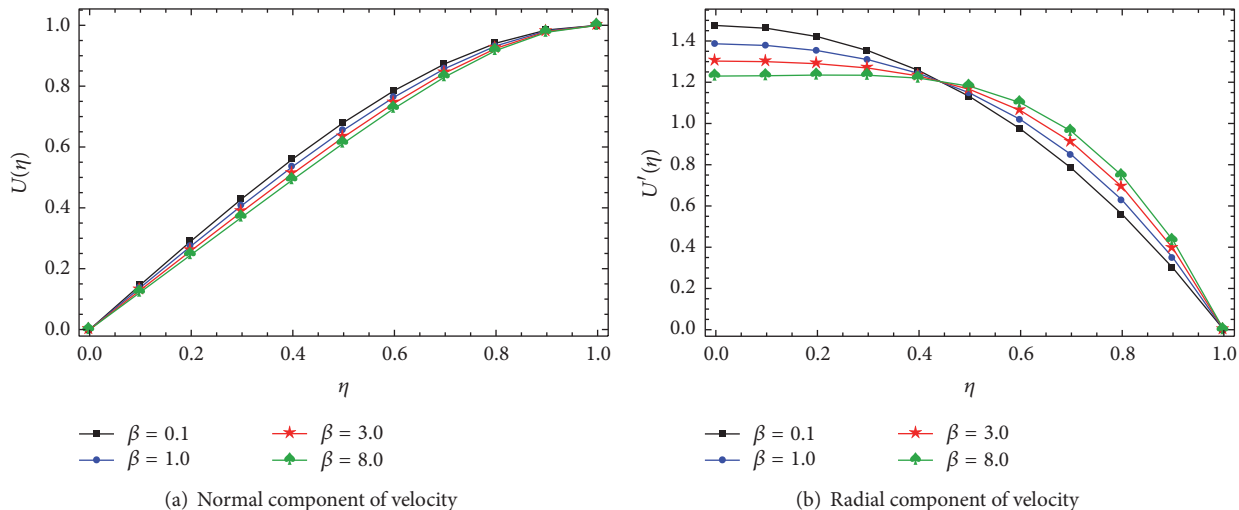
FIGURE 8: Effect of Casson parameter β on the velocity profile when S_q is positive.

(a) Normal component of velocity

(b) Radial component of velocity
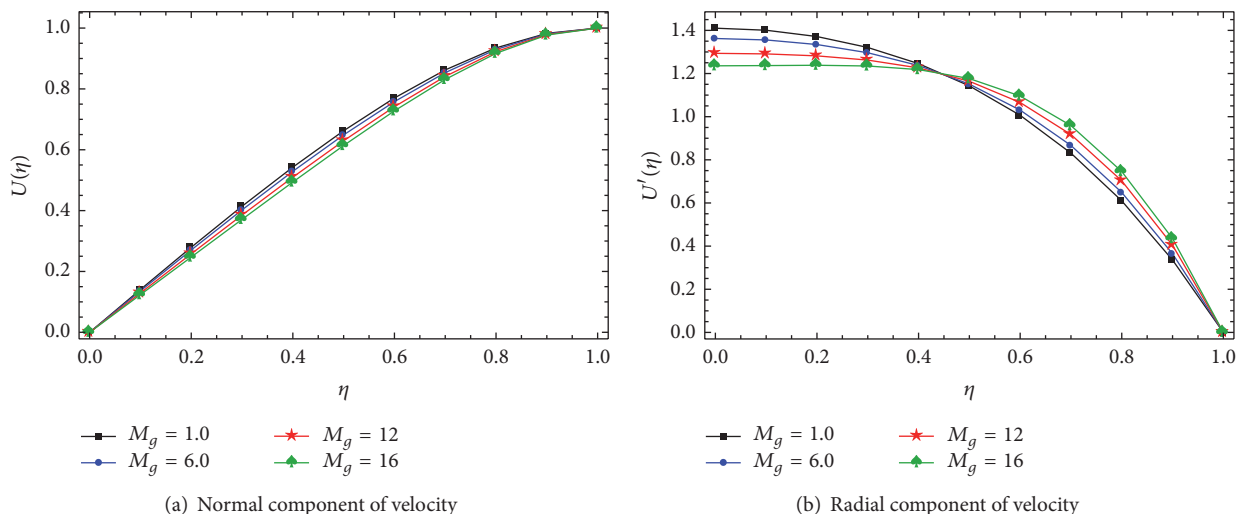
FIGURE 9: Effect of MHD parameter M_g on the velocity profile when S_q is positive.

(a) Normal component of velocity

(b) Radial component of velocity
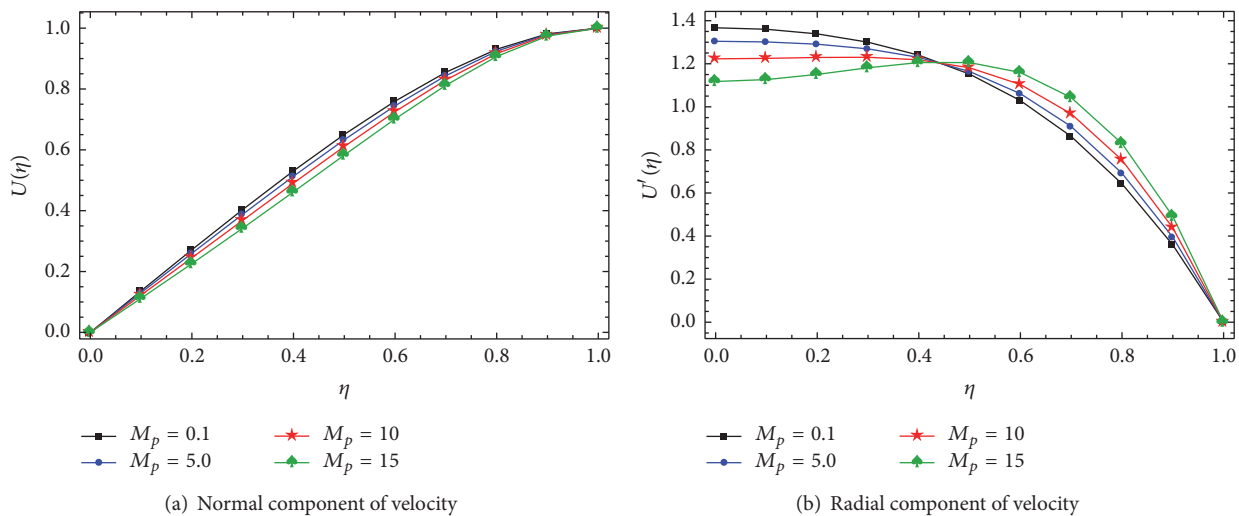
FIGURE 10: Effect of permeability constant M_p on the velocity profile when S_q is positive.

whereas the radial velocity increases near the lower plates and terminates near the upper plate. The effect when β is increased is similar to that of increasing negative S_q. Secondly, the effect of MHD parameter M_g is depicted in Figure 5. Here, it is seen that the normal component of the velocity decreases with the increase in M_g, while the radial component decreases near the lower plate and terminates near the upper plate. Moreover, the radial component of velocity decreases when $0 < \eta \leq 0.45$ and increases when $0.45 < \eta \leq 1$. Lastly, the effect of permeability parameter M_p is shown in Figure 6. Here, the normal velocity decreases when M_p is increased, while the radial velocity decreases near the lower plate and terminates near the upper plate. It can therefore be concluded from these observations that the effect of M_p and M_g is similar on the velocity profile in case of negative squeeze number.

The effect of $S_q > 0$ on the velocity profile is also investigated. In Figure 7, it is shown that the normal component of velocity decreases as S_q is increased, while the radial component of velocity decreases near the lower plate and terminates near the upper plate. Moreover, the radial velocity decreases in the interval $0 < \eta \leq 0.45$ and increases in $0.45 < \eta \leq 1$. The next three figures show the effect of β, M_g, and M_p in case of positive squeeze number. First, the effect of β is illustrated in Figure 8, showing that the normal component of velocity decreases as β is increased, while the radial component decreases near the lower plate and terminates near the upper plate. The effect of M_g is shown in Figure 9, while that of M_p is shown in Figure 10. In both cases, a similar effect as that of β can be observed.

In summary, it can be observed that positive and negative S_q have opposite effects on the velocity profile. Moreover, β shows opposite effect on the velocity profile in case of positive and negative S_q. However, M_g and M_p have similar effects on the velocity profile irrespective of the sign of the squeeze number. It is also observed that S_q, M_g, and M_p have similar effect while β has opposite effect on the skin friction coefficient.

6. Conclusion

This article presents a similarity solution for an unsteady squeezing flow of the non-Newtonian Casson fluid with MHD effect and passing through porous medium. The PDEs were reduced to a highly nonlinear fourth-order ODE by applying similarity transformations and then solved using the Homotopy Perturbation Method (HPM) and the fourth-order explicit Runge-Kutta method. Convergence and validity of the obtained solution was confirmed and found to be in good agreement. A comprehensive analysis was also performed to investigate the effect of various fluid factors like squeeze number, Casson, permeability, and MHD parameters on the velocity profile.

Appendix

Φ_{1i}, $i = 1, 2, \ldots, 6$ are the coefficients of various powers of η in first-order solution:

$$
\begin{aligned}
\Phi_{11} &= 168M_p\beta + 168M_g\beta + 419S_q\beta, \\
\Phi_{12} &= 336M_p\beta + 336M_g\beta + 873S_q\beta, \\
\Phi_{13} &= 168M_p\beta + 168M_g\beta + 504S_q\beta, \\
\Phi_{14} &= 28S_q\beta, \\
\Phi_{15} &= 24S_q\beta, \\
\Phi_{16} &= 2S_q\beta.
\end{aligned}
\tag{A.1}
$$

Φ_{2j}, $j = 1, 2, \ldots, 11$ are the coefficients of various powers of η in second-order solution:

$$
\Phi_{21} = \begin{cases} -12684672M_p^2\beta^2 - 25369344M_pM_g\beta^2 - 12684672M_g^2\beta^2 \\ -92692600M_pS_q\beta^2 - 92692600M_gS_q\beta^2 - 154163807S_q^2\beta^2, \end{cases}
$$

$$
\Phi_{22} = \begin{cases} 31135104M_p^2\beta^2 + 62270208M_pM_g\beta^2 + 31135104M_g^2\beta^2 \\ +205741536M_pS_q\beta^2 + 205741536M_gS_q\beta^2 + 324472661S_q^2\beta^2, \end{cases}
$$

$$
\Phi_{23} = \begin{cases} -24216192M_p^2\beta^2 - 48432384M_pM_g\beta^2 - 24216192M_g^2\beta^2 \\ -135567432M_pS_q\beta^2 - 135567432M_gS_q\beta^2 - 188756568S_q^2\beta^2, \end{cases}
$$

$$
\Phi_{24} = \left\{ 672672M_pS_q\beta^2 + 672672M_gS_q\beta^2 + 1677676S_q^2\beta^2, \right.
$$

$$
\Phi_{25} = \begin{cases} 5765760M_p^2\beta^2 + 11531520M_pM_g\beta^2 + 5765760M_g^2\beta^2 \\ +24216192M_pS_q\beta^2 + 24216192M_gS_q\beta^2 + 17976816S_q^2\beta^2, \end{cases}
$$

$$
\Phi_{26} = \left\{ -1009008M_pS_q\beta^2 - 1009008M_gS_q\beta^2 + 332046S_q^2\beta^2, \right.
$$

$$
\Phi_{27} = \left\{ -1441440M_pS_q\beta^2 - 1441440M_gS_q\beta^2 - 1441440S_q^2\beta^2, \right.
$$

$$
\Phi_{28} = \left\{ +80080M_pS_q\beta^2 + 80080M_gS_q\beta^2, \right.
$$

$$
\Phi_{29} = 109928S_q^2\beta^2,
$$

$$\Phi_{210} = 12376 S_q^2 \beta^2,$$

$$\Phi_{211} = 168 S_q^2 \beta^2.$$

(A.2)

Competing Interests

There are no competing interests regarding the publication of this paper.

References

[1] E. W. Mrill, A. M. Benis, E. R. Gilliland, T. K. Sherwood, and E. W. Salzman, "Pressure-flow relations of human blood in hollow fibers at low flow rates," *Journal of Applied Physiology*, vol. 20, no. 5, pp. 954–967, 1965.

[2] D. A. McDonald, *Blood Flows in Arteries*, Arnold, London, UK, 2nd edition, 1974.

[3] H. I. Andersson and B. S. Dandapat, "Flow of a powerlaw fluid over a stretching sheet," *Applied Analysis of Continuous Media*, vol. 1, no. 339, 1992.

[4] M. Sajid, I. Ahmad, T. Hayat, and M. Ayub, "Unsteady flow and heat transfer of a second grade fluid over a stretching sheet," *Communications in Nonlinear Science and Numerical Simulation*, vol. 14, no. 1, pp. 96–108, 2009.

[5] N. Casson, *Rheology of Dispersed System*, vol. 84, Pergamon Press, Oxford, UK, 1959.

[6] R. K. Dash, K. N. Mehta, and G. Jayaraman, "Casson fluid flow in a pipe filled with a homogeneous porous medium," *International Journal of Engineering Science*, vol. 34, no. 10, pp. 1145–1156, 1996.

[7] N. T. M. Eldabe and M. G. E. Salwa, "Heat transfer of mhd non-newtonian casson fluid flow between two rotating cylinder," *Journal of the Physical Society of Japan*, vol. 64, p. 4164, 1995.

[8] M. H. Hamdan, "An alternative approach to exact solutions of a special class of Navier-Stokes flows," *Applied Mathematics and Computation*, vol. 93, no. 1, pp. 83–90, 1998.

[9] M. H. Hamdan and F. M. Allan, "A note on the generalized Beltrami flow through porous media," *International Journal of Pure and Applied Mathematics*, vol. 27, no. 4, pp. 491–500, 2006.

[10] K. Vafai and C. L. Tien, "Boundary and inertia effects on flow and heat transfer in porous media," *International Journal of Heat and Mass Transfer*, vol. 24, no. 2, pp. 195–203, 1981.

[11] S. Islam, M. R. Mohyuddin, and C. Y. Zhou, "Few exact solutions of non-Newtonian fluid in porous medium with hall effect," *Journal of Porous Media*, vol. 11, no. 7, pp. 669–680, 2008.

[12] K. Vafai, *Handbook of Porous Media*, CRC Press, Taylor and Francis, Boca Raton, Fla, USA, 2nd edition, 2005.

[13] S. Abbasbandy, "A new application of He's variational iteration method for quadratic Riccati differential equation by using Adomian's polynomials," *Journal of Computational and Applied Mathematics*, vol. 207, no. 1, pp. 59–63, 2007.

[14] M. A. Abdou and A. A. Soliman, "Variational iteration method for solving BURger's and coupled BURger's equations," *Journal of Computational and Applied Mathematics*, vol. 181, no. 2, pp. 245–251, 2005.

[15] J.-H. He, "Homotopy perturbation technique," *Computer Methods in Applied Mechanics and Engineering*, vol. 178, no. 3-4, pp. 257–262, 1999.

[16] J.-H. He, "A coupling method of a homotopy technique and a perturbation technique for non-linear problems," *International Journal of Non-Linear Mechanics*, vol. 35, no. 1, pp. 37–43, 2000.

[17] J.-H. He, "Homotopy perturbation method for solving boundary value problems," *Physics Letters. A*, vol. 350, no. 1-2, pp. 87–88, 2006.

[18] A. M. Siddiqui, R. Mahmood, and Q. K. Ghori, "Thin film flow of a third grade fluid on a moving belt by He's homotopy perturbation method," *International Journal of Nonlinear Sciences and Numerical Simulation*, vol. 7, no. 1, pp. 7–14, 2006.

[19] N. Herişanu and V. Marinca, "Optimal homotopy perturbation method for a non-conservative dynamical system of a rotating electrical machine," *Zeitschrift fur Naturforschung A*, vol. 67, no. 8-9, pp. 509–516, 2012.

[20] F. Wang, W. Li, and H. Zhang, "A new extended homotopy perturbation method for nonlinear differential equations," *Mathematical and Computer Modelling*, vol. 55, no. 3-4, pp. 1471–1477, 2012.

[21] A. Nazari-Golshan, S. S. Nourazar, H. Ghafoori-Fard, A. Yildirim, and A. Campo, "A modified homotopy perturbation method coupled with the Fourier transform for nonlinear and singular Lane-Emden equations," *Applied Mathematics Letters*, vol. 26, no. 10, pp. 1018–1025, 2013.

[22] M. Qayyum and H. Khan, "Behavioral study of unsteady squeezing flowthrough porous medium," *Journal of Porous Media*, vol. 19, no. 1, pp. 83–94, 2016.

[23] M. Qayyum, H. Khan, M. T. Rahim, and I. Ullah, "Modeling and analysis of unsteady axisymmetric squeezing fluid flow through porous medium channel with slip boundary," *PLoS ONE*, vol. 10, no. 3, Article ID e0117368, 2015.

[24] H. Aminikhah, "The combined Laplace transform and new homotopy perturbation methods for stiff systems of ODEs," *Applied Mathematical Modelling*, vol. 36, no. 8, pp. 3638–3644, 2012.

[25] U. Filobello-Nino, H. Vazquez-Leal, B. Benhammouda et al., "Nonlinearities distribution Laplace transform-homotopy perturbation method," *SpringerPlus*, vol. 3, article 594, 2014.

[26] M. Mustafa, T. Hayat, and S. Obaidat, "On heat and mass transfer in the unsteady squeezing flow between parallel plates," *Meccanica*, vol. 47, no. 7, pp. 1581–1589, 2012.

[27] M. Esmaeilpour and D. D. Ganji, "Solution of the Jeffery-Hamel flow problem by optimal homotopy asymptotic method," *Computers & Mathematics with Applications*, vol. 59, no. 11, pp. 3405–3411, 2010.

[28] A.-M. Wazwaz, "Approximate solutions to boundary value problems of higher order by the modified decomposition method," *Computers & Mathematics with Applications*, vol. 40, no. 6-7, pp. 679–691, 2000.

[29] M. Aslam Noor and S. T. Mohyud-Din, "Variational iteration technique for solving higher order boundary value problems," *Applied Mathematics and Computation*, vol. 189, no. 2, pp. 1929–1942, 2007.

[30] J. C. Butcher, "A history of Runge-Kutta methods," *Applied Numerical Mathematics*, vol. 20, no. 3, pp. 247–260, 1996.

[31] O. Khan, F. Khan, C. Ragusa, and B. Montrucchio, "Review of parallel and distributed architectures for micromagnetic codes," *COMPEL*, vol. 32, no. 6, pp. 1891–1900, 2013.

[32] S. Nadeem, R. Mehmood, and N. S. Akbar, "Oblique stagnation point flow of a casson-nano fluid towards a stretching surface with heat transfer," *Journal of Computational and Theoretical Nanoscience*, vol. 11, no. 6, pp. 1422–1432, 2014.

[33] M. Nakamura and T. Sawada, "Numerical study on the laminar pulsatile flow of slurries," *Journal of Non-Newtonian Fluid Mechanics*, vol. 22, no. 2, pp. 191–206, 1966.

[34] C.-Y. Wang, "The squeezing of a fluid between two plates," *Journal of Applied Mechanics*, vol. 43, no. 4, p. 579, 1976.

[35] U. Khan, N. Ahmed, S. I. U. Khan, S. Bano, and S. T. Mohyuddin, "Unsteady squeezing flow of a casson fluid between parallel plates," *World Journal of Modelling and Simulation*, vol. 10, no. 4, pp. 308–319, 2014.